TECHNICAL MEMORANDUMS

NATIONAL ADVISORY COMMITTEE FOR AERONAUTICS

No. 820

SOME EXPERIMENTS ON THE SLIPSTREAM EFFECT

By C. Ferrari

Aeronautical Laboratory of
the Royal Engineering Institute of Turin

Washington
March 1937

NATIONAL ADVISORY COMMITTEE FOR AERONAUTICS

TECHNICAL MEMORANDUM NO. 820

SOME EXPERIMENTS ON THE SLIPSTREAM EFFECT*

By C. Ferrari

"Torino (30-31-32)" and "Torino El" (figs. 1-19).- The models designated "Torino 30, 31, 32" are horizontal tail surfaces of rectangular, triangular, and elliptical plan form and all of the same profile section, as indicated in figure 1. The geometrical characteristics of "Torino El" are shown in figure 2. The tests on these models were carried out under the initiative of General Crocco following a request by the Ministry of Aeronautics, the object being to determine the effect of the propeller slipstream on the aerodynamical characteristics of the horizontal stabilizer. The results which are here presented correspond to a first series of tests made without an interposed wing and in which the distance between the plane of the propeller disk and the tail was maintained constant. Other tests which are now being conducted are devoted to a study of the effect on the tail interference brought about by either varying the distance between the propeller and wing or placing a wing at different positions between the stabilizer and propeller. The test set-up is shown in figure 3.

The propeller, of diameter D = 600 millimeters equal to the span of the tail surfaces tested, and of pitch p = 540 millimeters measured at 0.785 radius, is mounted on the propeller balance described in the first series of these reports and which permits the propeller axis to be set at any angle of yaw with respect to the wind direction. The stabilizer, by means of a rigid arm, is supported on the universal balance having three fulcrums, described in "Il Laboratorio di Aeronautica del R. Politecnico di Torino" (Journal of the National Association of Italian Engineers, 1920) by the director of the laboratory, Professor Panetti, and is arranged with the plane of symmetry horizontal (the span therefore vertical). In order to be able to keep the relative position of the tail with respect to the propeller unchanged at any deflection and measure the rolling moments exerted on the tail surface by the action of the propeller, the latter was suspended in the wind tunnel in the following manner: The vertical arm A of the

*Experimental Reports by the Aeronautical Laboratory of the Royal Engineering Institute of Turin, Series 2, pp. 38-55.

balance which transmits the aerodynamic forces to the balance carries a horizontal sleeve B, which in turn supports on ball bearings a horizontal tube C through which there runs shaft D terminating in horizontal tube E, normal to D. Within tube E runs the rod F which may thus be set at any horizontal distance from the tunnel axis. The rod F has a circular slot opening within which moves the circular sector H to which the model is rigidly attached. By thus combining the rotation about the vertical axis L with the horizontal displacements along E and D, the displacement of the stabilizer may be reduced to a rotation about the same vertical axis K about which the propeller is made to turn to give the desired angle of yaw α. Pressure and stop screws permit the model to be fixed in any position. Since the horizontal tube C which supports the shaft bearing the model is borne by sleeve B fixed to the balance arm by ball bearing, the rolling moment is measured by another balance to which the moment is transmitted by wires at the ends of a horizontal rod carried by shaft D.

For each angle of yaw α of the propeller axis with respect to the wind direction there were measured the lift and the rolling moments of the tail, the coefficient of the thrust and torque, and the side force and corresponding torque due to the deviation of the thrust line from the wind direction and the measurements were taken over the entire range of values of γ between zero and maximum aerodynamic pitch. No determinations were made of the tail drag because the thrust was sufficiently large compared to the drag of the model to make the measurement of the latter of little importance. The torque and force coefficients of the propeller at various angles of yaw were determined by the method indicated by the director of the laboratory in the first of these series of reports. The measurement of the lift of the tail was obtained with the three-fulcrum balance with the rigid arm, while the rolling moments were measured with the wire balance with the model mounted as above described. The results of the tests are shown for the propeller in figures 4, 5, 6, and 7, and for the stabilizers in figures 8, 9, 10, 11, 15, 16, 17, and 18.

From the curves of figures 4 and 5 it may be seen that the angle α has the effect of increasing the thrust coefficient τ and the torque coefficient κ but if angles not greater than 20° are considered and the same coefficients are referred not to $\gamma = V/\Omega R$ but to $\gamma_e = V \cos \alpha/\Omega R$ these increases, as may be seen from figures

6 and 7, are small enough to be neglected, in complete agreement with the theoretical prediction. Thus, for example, the increase in τ corresponding to $\alpha = 20^0$ is barely 9 percent for $\gamma_e = 0.3$, and 3.8 percent for $\gamma_e = 0.2$, while the increase in κ is 6.1 percent for $\gamma_e = 0.25$. A slight discrepancy is shown on the diagram of κ as a function of α for $\gamma_e = 0.3$.

The side thrust coefficients h vary for each value of γ_e in the above range of α almost linearly with α as figure 6 shows and the slopes $(\partial h/\partial \alpha)_{\gamma_e = \text{const}}$ obtained experimentally agree quite well with those deducible from the theory of a propeller yawed to the wind direction.

This is, in fact, the reason that the coefficient of side thrust (reference 1) h may be put in the form $h = h_D \frac{S}{R^2}$ where S is the total blade area of the propeller of radius R and h_D is given by

$$h_D = \frac{1}{2} \gamma_o [\gamma_o c_\infty' \zeta \varphi_o + c_o (\psi_o + \theta_1)] \quad (8)$$

where, in accordance with the usual symbols adopted in the theory of Professor Pistolesi

$$\gamma = \frac{V}{\Omega R}; \quad \text{in which} \quad \gamma_o = \gamma \frac{1 + \frac{v}{V}}{1 - \frac{\omega}{\Omega}}$$

putting $\cos \alpha_e = 1$; v and ω being the induced axial and rotational increments; c_∞' is the angular coefficient of lift for infinite span and in the developed computation may be put equal to 2.8; ζ is the value of γ_o corresponding to the aerodynamic pitch of the propeller. φ_o, ψ_o, and θ_1 are the functions of ζ introduced by Professor Pistolesi in the above theory and whose values corresponding to the various values of ζ are tabulated in Pistolesi's paper "A Simplified Theory for the Study of Propellers" (Rendiconti Tecnici e sperimentali di Aeronautico, March 1923) and in the paper by the same author "Effect of Angle of Yaw on the Propeller Characteristics" (L'Aerotecnica, 1925). (See also Panetti, reference 1.) (8) is the tangent of the effective angle of yaw α_e corresponding to the apparent angle α and for the range of α considered may be assumed as equal to the value of the angle α_e itself, while $\cos \alpha_e$ may be put equal to 1, so that

$$\alpha_e = \alpha - \frac{x}{2\,(V + v)}$$

where x is the increment normal to V induced by the propeller at infinity.

The increments x and v corresponding to definite values of γ and α are determined without difficulty by means of the theorems of the change in momentum of the mass affected by the propeller along and normal to V. There are obtained, respectively (reference 2):

$$\left.\begin{aligned} \pi R^2 \rho \left[(V+v)\cos\alpha - \frac{x}{2}\sin\alpha\right] 2v &= T\cos\alpha - H\sin\alpha = \\ &= \rho R^4 \Omega^2 (\tau\cos\alpha - h\sin\alpha) \\ \pi R^2 \rho \left[(V+v)(1+\cos\alpha) - \frac{x}{2}\sin\alpha\right] x &= \rho R^4 \Omega^2 (\tau\sin\alpha + h\cos\alpha) \end{aligned}\right\} (1)$$

In the first of equations (1) if $\frac{x}{2V}\sin\alpha$ is neglected in comparison with $(1 + v/V)\cos\alpha$ as may justifiably be done in view of the order of magnitude of the values of α and $x/2V$, there is obtained:

$$\frac{v}{V} = \sqrt{\frac{\tau - h\tan\alpha}{2\pi\gamma^2} + \frac{1}{4}} - \frac{1}{2} = \sqrt{\frac{\tau_o}{2\pi\gamma^2} + \frac{1}{4}} - \frac{1}{2} \qquad (2)$$

where $\tau_o = \tau - h\tan\alpha$. It is important to note that τ_o is likewise to a close approximation the coefficient of thrust of the propeller <u>without yaw</u> corresponding to the same value of γ. The correction term for τ for an incidence of the propeller disk α is, in fact,

$$t_D \frac{S}{R^2} = \frac{S}{R^2}\frac{1}{2}\gamma_o^2 \, c_{\infty}' \, \zeta \, \varphi_o(\delta)$$

which coincides with expression $h\tan\alpha$ except for terms like that containing the coefficient of form drag whose order of magnitude is small enough to be negligible. It is thus permissible to calculate the increment in the velocity as though the propeller were not yawed to the wind direction provided that the increment is disposed not along the propeller axis but along the asymptotic wind direction. This important property is confirmed by the test results as shown in table I.

From the second of equations (1), we thus have:

$$\frac{x}{V} = \frac{\tau \sin \alpha + h \cos \alpha}{\pi \gamma^2 (1 + \cos \alpha)\left(1 + \frac{v}{V}\right)} \tag{3}$$

so that

$$\alpha_e = \alpha - \frac{x}{2V} = \alpha - \frac{\tau \alpha + \frac{S}{R^2} f(\gamma) \alpha_e}{4\pi \gamma^2 \left(1 + \frac{v}{V}\right)} \tag{4}$$

where γ is the apparent velocity ratio corresponding to the effective ratio γ_o and

$$f(\gamma) = \tfrac{1}{2} \gamma_o [\gamma_o c_\infty' \zeta \varphi_o + c_o (\psi_o + \theta_1)]$$

From equation (4) we obtain:

$$\alpha_e = \frac{1 - \frac{\tau}{4\pi \gamma^2 \left(1 + \frac{v}{V}\right)}}{1 + \frac{S}{R^2} \frac{f(\gamma)}{4\pi \gamma^2 \left(1 + \frac{v}{V}\right)}} \alpha = \frac{f_1(\gamma)}{f_2(\gamma)} \alpha$$

and therefore

$$h = \frac{S}{R^2} f(\gamma) \frac{f_1(\gamma)}{f_2(\gamma)} \alpha$$

$$\left(\frac{\partial h}{\partial \alpha}\right)_{\substack{\gamma = \text{const} \\ \alpha = 0}} = \frac{S}{R^2} f(\gamma) \frac{f_1(\gamma)}{f_2(\gamma)}$$

The above formulas were used for calculating the values of $\partial h / \partial \alpha$, putting $S/R^2 = 0.19$, $\zeta = 0.335$, and assuming:

$c_\infty' = 2.8$, $c_o = 0.01$, $\varphi_o = 1.467$, $\theta_1 = 0.425$, $\psi_o = 0.62$.

The computations are given in the table below.

γ	τ	γ_o	$f(\gamma)$	$f_1(\gamma)$	$f_2(\gamma)$	$\frac{\partial h}{\partial \alpha}$ calculated	$\frac{\partial h}{\partial \alpha}$ experimental
0.3	0.0055	0.303	0.0635	0.99	1.0180	0.0118	0.0114
.25	.0167	.263	.048	.96	1.022	.0086	.0083
.2	.025	.226	.0365	.91	1.02	.0062	.0064
.15	.0288	.178	.023	.835	1.025	.0035	.0042

The agreement between the computed and test results shown in the last column of the table appears to be very good even for the smallest values of γ. The importance of this result, as brought out on figures 6 and 7, showing the effect of α on the coefficients τ and k, lies essentially in the possibility of determining the aerodynamic elements of the propeller, necessary for the computation of the interference of the latter on the other airplane parts, from the propeller characteristics calculated or derived experimentally for zero angle between thrust line and wind direction.

The effect which the propeller slipstream produces on the lift of the tail is clearly shown in figures 8-11. It is immediately evident that the increment in the lift increases as γ decreases. The relative increment decreases, however, at larger angles α. a fact which may at least qualitatively be explained if it is observed that the portion of the stabilizer which lies in the propeller slipstream is smaller the larger the angle α.

In order to obtain a good interpretation of the test results, it is convenient to compare the results with those obtainable by the theory based on the consideration of a perfect fluid in which the damping of the vortices and the resulting deformation of the propeller wake is not considered.

If, in the determination of the lift of the tail, the rotational increments induced by the propeller are not taken into account, these increments producing essentially a dissymmetry in the distribution of the circulation along the stabilizer span, and the stabilizer is assumed to be completely immersed in the propeller slipstream, the lift coefficient c_p becomes

$$c_p = c_{p_o}' \left(1 + \frac{2v}{V}\right)^2 (\alpha - \alpha_{i_e})$$

where c_{p_o}' is the angular lift coefficient of the tail surface for the locked propeller and therefore zero increment v while α_{i_e} denotes the change in the incidence on the tail resulting from the propeller action. But

$$\alpha_{i_e} = \frac{x}{V\left(1 + \frac{2v}{V}\right)}$$

where x is the increment defined above normal to V. We obtain:

$$c_p = c_{p_o}\left(1 + \frac{2v}{V}\right)^2 - c_{p_o}' \frac{x}{V}\left(1 + \frac{2v}{V}\right) \qquad (5)$$

The first term of the second member of (5) in which c_{p_o} is the coefficient of lift of the tail with propeller locked, defines the effect of the increment in velocity produced by the propeller while the second term corresponds to the effect of the wind deviation. Equation (5) is identical in form with the stability formula of G. A. Crocco (reference 3), giving the interference of the propeller on the stabilizer.

The values of the increments 2v/V and x/V, corresponding to the various angles α at which the tests were conducted, were computed for the values of γ equal to 0.30, 0.25, 0.20, 0.15, 0.10 by means of formulas (2) and (3) and from the diagrams of figures 4 and 5. The results of the computations are given in table I, in which are also indicated the computed values of c_p and compared with those determined experimentally. The diagrams for the calculated values of c_p have been drawn on figures 8 and 11. From these it may be seen that the agreement between theory and experiment is sufficiently good on the average until angles above 10° are considered. The reason for the appreciable departure of the theoretical from the experimental results at the higher angles is immediately evident on examination of figure 14 showing the wake or slipstream for angles α of 15° and 20°. It is seen that for $\alpha = 15°$ about 40 percent of the tail is outside the slipstream. The theoretical determination of the aerodynamic characteristics of the stabilizer under these conditions is extremely difficult, chiefly on account of the phenomenon of diffusion and extinction of the vorticity as a result of the viscosity. It is nevertheless easy to see that there would be a very strong decrease in the velocity increment and therefore in the lift of the tail. This is further confirmed by the fact that the angle at which maximum lift occurs is smaller the smaller the value of γ (figs. 8 and 11).

In order to give a better comparison of the experimental results with those of the simplified theory developed, it is convenient to put equation (5) in a different form. It is seen from figure 12 where the angles of deviation

x/V, are plotted for various values of γ against the angles of yaw α, that in complete agreement with the theory of a yawed propeller, in the range of incidences considered,

$$\frac{x}{V} = \varphi(\gamma)\ \alpha \tag{6}$$

that is, the angle of deviation of the flow for each value of the ratio γ is proportional to the angle of yaw α. The values of $\varphi(\gamma)$ for each value of γ are given in figure 12 and table II.

Substituting now in equations (5) and (6) and denoting by β the angle that the line of zero lift of the tail makes with the propeller axis, we have:

$$c_p = c_{p_o}' \left(1 + \frac{2v}{V}\right)^2 \left[\alpha \left(1 - \frac{\varphi(\gamma)}{1 + \frac{2v}{V}}\right) + \beta\right]$$

from which the result is obtained that the lift coefficient of the stabilizer in the presence of the propeller for every constant value of γ is

$$c_p' = c_{p_o}' \left(1 + \frac{2v}{V}\right)^2 \left(1 - \frac{\varphi(\gamma)}{1 + \frac{2v}{V}}\right) = c_{p_o}' \left(1 + \frac{2v}{V}\right)^2 [1 - \varphi_1(\gamma)] \tag{7}$$

while the increment in the angle of zero lift is

$$\Delta\epsilon = \beta \frac{\varphi(\gamma) \frac{1}{1 + \frac{2v}{V}}}{1 - \frac{\varphi(\gamma)}{1 + \frac{2v}{V}}} = \beta \frac{\varphi_1(\gamma)}{1 - \varphi_1(\gamma)} \tag{8}$$

where

$$\varphi_1(\gamma) = \varphi(\gamma) \frac{1}{1 + \frac{2v}{V}}$$

The values of c_p' and $\Delta\epsilon$ calculated by the above formulas are compared with the experimental values in table II and figure 13. It may be seen that the agreement is better for the deviation $\Delta\epsilon$ of the angle of zero lift and hence for the deviation of the flow produced by the pro-

peller than for the coefficient c_p'. For the latter the approximation of the theoretical results is good only for $\gamma \leq 0.25$.

Figures 15-18 give the coefficients of rolling moment c_{mr} defined by

$$c_{mr} = \frac{M_r}{\rho S V^2 l_m} \tag{9}$$

in which l_m is the mean chord of the stabilizer

$$(l_{mr} = \text{area}/\text{span})$$

as a function of the incidence α for the various values of γ already considered. The rolling moments, as has already been noted, result from the velocity increments produced by the propeller and which at two wing sections at equal distances from the plane of symmetry determine increments $\Delta\alpha$ that may be assumed equal and opposite; i.e., for an element at distance r from the said plane, if ω is the induced angular velocity increment $\Delta\alpha = \pm \frac{r\omega}{V + 2v}$. There is thus obtained for the rolling moment over the entire tail area:

$$M_r = 2\rho V \int_0^R c_p' l r^2 \omega \left(1 + \frac{2v}{V}\right) dr = \rho \frac{V^2 DS}{\gamma} \bar{h} c_p' \frac{\omega}{\Omega} \left(1 + \frac{2v}{V}\right) \tag{10}$$

where $\bar{h}$ is a constant whose value depends on the distribution law of the increments induced by the propeller along the tail span and also on the tail plan form, while D denotes the propeller diameter. Substituting the expression for M_r given by (10), there is obtained:

$$c_{mr} = \frac{D}{l_m} \frac{c_p'}{\gamma} \bar{h} \frac{\omega}{\Omega} \left(1 + \frac{2v}{V}\right) = \frac{D}{l_m} \frac{c_{p_o}'}{\gamma} \left[1 - \varphi_1(\gamma)\right] \bar{h} \frac{\omega}{\Omega} \left(1 + \frac{2v}{V}\right) \tag{11}$$

The mean increments ω/Ω may be computed by means of the equation

$$\frac{\omega}{\Omega} = \frac{2\kappa}{\pi} \frac{1}{\gamma \cos \alpha \left(1 + \frac{v}{V}\right)} \tag{12}$$

Applying equation (11) for the determination of the coefficients c_{mr} for $\alpha = 0$ and putting for the values

of c_{mr} those given by the tests and which result from figures 15 and 18, there are obtained the values of $\bar{h}$ given in the table below. It is immediately evident that the variations in the constant $\bar{h}$ due either to variations of γ or of the plan form are rather small except near the value of $\gamma = 0.3$ which is near the aerodynamic pitch of the propeller. It should likewise be observed that for the rectangular tail the value of $\bar{h}$ would be $\bar{h} = 1/6 = 0.167$ if the lift were uniform along the span and the increments induced by the propeller were likewise constant.

γ		0.3	0.25	0.20	0.15
$1000\ \kappa$		2.4	4.95	6.2	6.7
$1000\ \frac{\omega}{\Omega}$		5.1	12.2	18.4	24.2
c_{mr},	rectangular stabilizer	.025	.034	.055	.105
c_{mr},	elliptical stabilizer	.024	.032	.052	.103
c_{mr},	triangular stabilizer	.02	.03	.046	.083
$\bar{h}$	rectangular stabilizer	.278	.127	.105	.105
$\bar{h}$	elliptical stabilizer	.278	.127	.105	.105
$\bar{h}$	triangular stabilizer	.243	.122	.096	.091

As α increases, according to equation (11), the coefficients would remain constant if it were not for small variations in ω/Ω due to the yaw of the propeller, for all the values of α corresponding to the straight-line portion of the lift curve. The test curves are in fact horizontal tangents for $\alpha = 0$ and decrease rapidly for an angle of incidence that is less than the critical. This is a consequence of the fact already pointed out that as the yaw angle α increases, an increasingly larger portion of the stabilizer lies outside the propeller slipstream and that portion being further removed from the axis has the maximum efficiency as far as producing the rolling moment is concerned. The moment which was to the right reverses, although always remaining very small, for a value of α less than 10° at $\gamma = 0.30$ while the knee of the lift curve lies at less than 16°. This also explains the very large values of $\bar{h}$ for values of γ near γ_s corresponding to the aerodynamic pitch. In the neighborhood of

$\omega = 0$ the ratio of the maximum to the mean increment increases rapidly because for one part of the radius the increment changes sign for a value of γ near but less than γ_s.

If it is desired to take account of the circumstance that the plane of the tail is not completely immersed in the propeller slipstream, it is necessary to multiply the coefficient c_{mr} given by equation (11) by the reduction factor

$$\Delta = \left[1 - \frac{L^2}{R}\frac{\alpha^2}{}\left[1 - \varphi_1(\gamma)\right]^2\right]^{3/2}$$

where L is the distance of the stabilizer from the propeller disk. It is thus seen that the decrease in the rolling-moment coefficient is at least qualitatively given by the theoretical formula.

It is still of interest to express the rolling moments on the tail caused by the rotational increments induced by the propeller as a function of the engine torque C applied to the propeller. We obtain:

$$\mu = \frac{M_r}{C} = \frac{c_{mr}\, S\, l_m}{\kappa R^3}\gamma^2$$

The other tests in the program undertaken by the Aeronautical Laboratory were devoted, as has already been said above, to the determination of the effect of the propeller on the lift of the stabilizer in the presence of a wing placed at different positions with respect to the propeller and with different positions of the stabilizer. The results of these tests, which were carried out on the apparatus described in the Experimental Reports, Series 1, and on the 6-component balance described in this paper, will be presented in a later series of these reports.

Translation by S. Reiss,
National Advisory Committee
for Aeronautics.

REFERENCES

1. Pistolesi, E.: Influsso di un vento laterale sul funzionamento delle eliche. L'Aerotecnica, 1925.

Panetti, M.: Corso di Costruzioni Aeronautiche.

2. Pistolesi, E.: Contributo allo studio dell'elica in un vento laterale. L'Aerotecnica, 1927.

Ferrari, C.: Sul problema dell'elica con vento laterale. L'Aerotecnica, 1928.

3. Crocco, G. A.: Elementi di Aviazione. Ministero dell'aeronautica, Rome, 1930, p. 573 and following.

TABLE I

α°	γ	τ	h	$1 + \frac{v}{V}$	$\frac{x}{V}$	Elevator setting 0°		Elevator setting 15°	
						Theoretical c_p	Experimental c_p	Theoretical c_p	Experimental c_p
0°	0.1	0.0305	0	1.357	-	-	-	0.616	0.55
	.15	.0288	0	1.174	-	-	-	.38	.375
	.20	.025	0	1.089	-	-	-	.291	.30
	.25	.0167	0	1.049	-	-	-	.245	.27
	.30	.0055	0	1.008	-	-	-	.216	.245
5°	0.1	0.0305	.0002	1.357	0.0335	0.3322	-	0.911	0.755
	.15	.0288	.00038	1.174	.0174	.2238	0.195	.5787	.58
	.20	.025	.0007	1.112	1.01039	.1801	.18	.545	.482
	.25	.0167	.0010	1.04	.0628	.158	.17	.3855	.425
	.30	.0055	.00137	1.009	.00322	.14568	.159	.349	.39
10°	0.10	0.0308	.00045	1.357	0.0682	0.636	-	1.186	0.84
	.15	.0293	.0009	1.175	.0362	.4215	0.35	.7675	.67
	.20	.0256	.0015	1.09	.0213	.337	.33	.6168	.59
	.25	.0177	.0021	1.042	.0127	.2929	.31	.5168	.55
	.30	.0067	.0029	1.01	.00708	.267	.295	.4695	.575
15°	0.10	0.031	.0008	1.358	0.1048	0.946	-	1.38	0.785
	.15	.0296	.0014	1.194	.0545	.618	0.385	.902	.632
	.20	.0265	.00225	1.10	.0333	.464	.36	.676	.565
	.25	.0192	.0033	1.044	.0203	.38	.345	.555	.532
	.30	.0088	.0045	1.013	.01185	.34	.34	.495	.505
20°	0.10	0.0315	.00118	1.36	0.1435	0.765	-	1.436	0.67
	.15	.0306	.00202	1.18	.0768	.5043	-	.8715	.52
	.20	.027	.00327	1.092	.0464	.3933	-	.6452	.47
	.25	.021	.0047	1.046	.0293	.3415	-	.5416	.455
	.30	.0115	.0065	1.016	.01815	.312	-	.4803	.45

TABLE II. Rectangular Surface

γ	Elevator setting 0° c_p' experimental	Elevator setting 15° c_p' experimental	Elevator setting 15° $\Delta\epsilon^\circ$ experimental	$1 + \frac{2v}{V}$	$\varphi(\gamma)$	$\varphi_1(\gamma)$	$1-\varphi_1(\gamma)$	$\Delta\epsilon^\circ$ calculated	c_p' calculated
∞	1.62	1.62	-	-	-	-	-	-	-
0.3	1.81	1.85	0.25	1.02	0.04	0.0392	0.9608	0.3	1.62
.25	1.95	1.97	.50	1.084	.075	.069	.931	.5	1.79
.2	2.1	2.09	.80	1.18	.126	.107	.893	.88	2.02
.15	2.24	2.35	1.6	1.348	.206	.153	.847	1.40	2.45
.10	-	3.2	2.9	1.714	.39	.228	.772	2.2	3.66

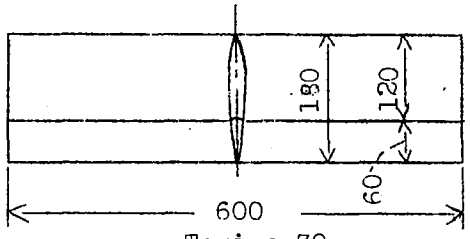

Torino 30

$S = 0.108\ m^2$

$L = \frac{S}{b} = 0.180m$

$\lambda = \frac{b^2}{S} = 3.3$

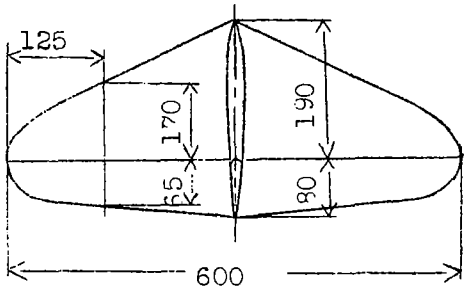

Torino 31

$S = 0.109\ m^2$

$L = \frac{S}{b} = 0.182m$

$\lambda = \frac{b^2}{S} = 3.3$

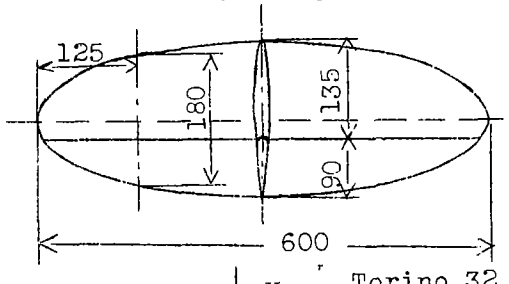

Torino 32

$S = 0.103\ m^2$

$L = \frac{S}{b} = 0.175m$

$\lambda = \frac{b^2}{S} = 3.5$

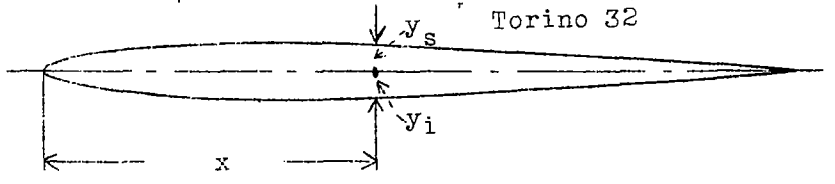

x	0	1.2	2	3.4	5	7	10	16	20
y_s	0	1.1	1.4	1.83	2.2	2.53	2.9	3.4	3.62
y_i									

x	30	40	50	60	70	80	90	94	100
y_s	3.98	3.9	3.46	2.7	2.12	1.42	0.73	0.42	0
y_i									

$C_p = \frac{F_p}{\rho S V^2}$ $C_r = \frac{F_r}{\rho S V^2}$ $C_{mr} = \frac{M_r}{\rho S L V^2}$

Figure 1.

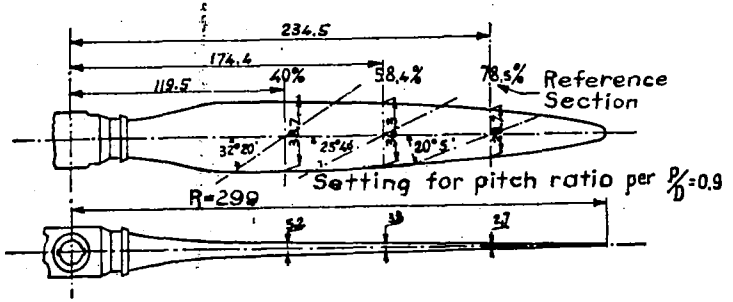

Figure 2.- Metal propeller with two adjustable blades. Torino E 1.

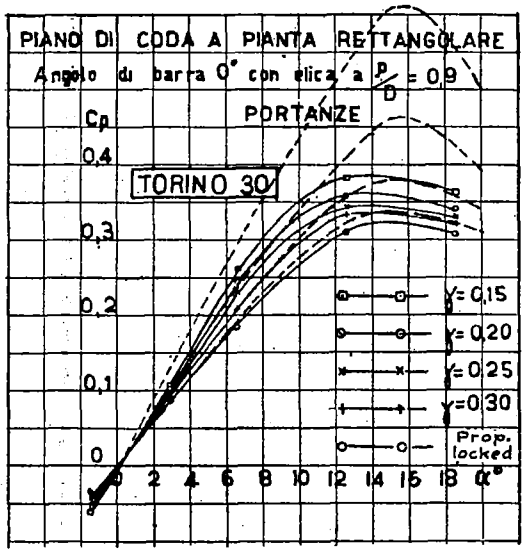

Figure 8.- Lift curves of tail of rectangular plan form. Torino 30.
Experimentally deduced curve.------
Angle of tail setting 0°. p/D=0.9

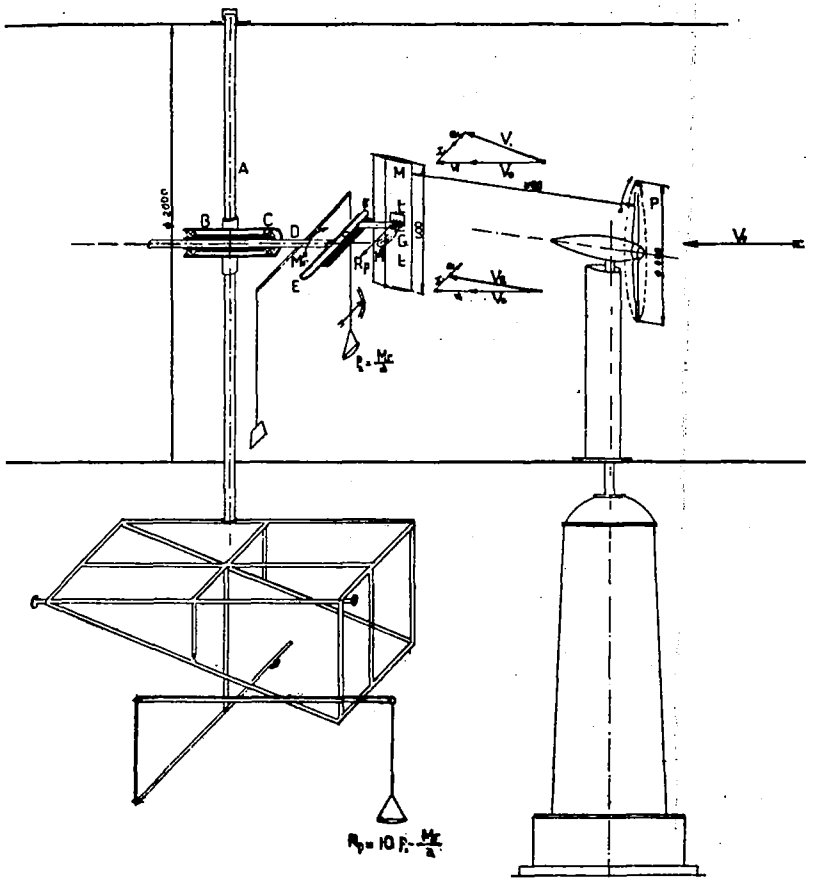

Figure 3.

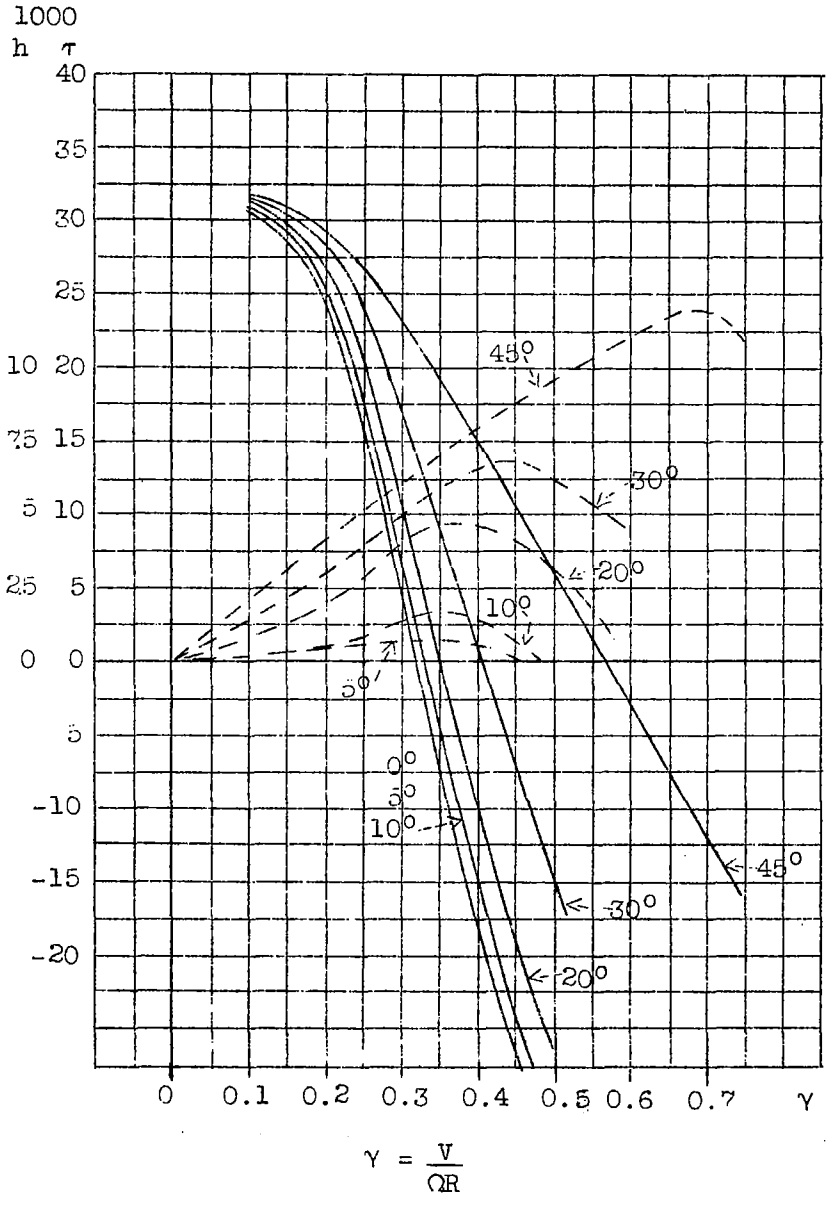

Figure 4.- Yaw tests, 2-blade metal propeller, Torino E 1. p/D= 0.9

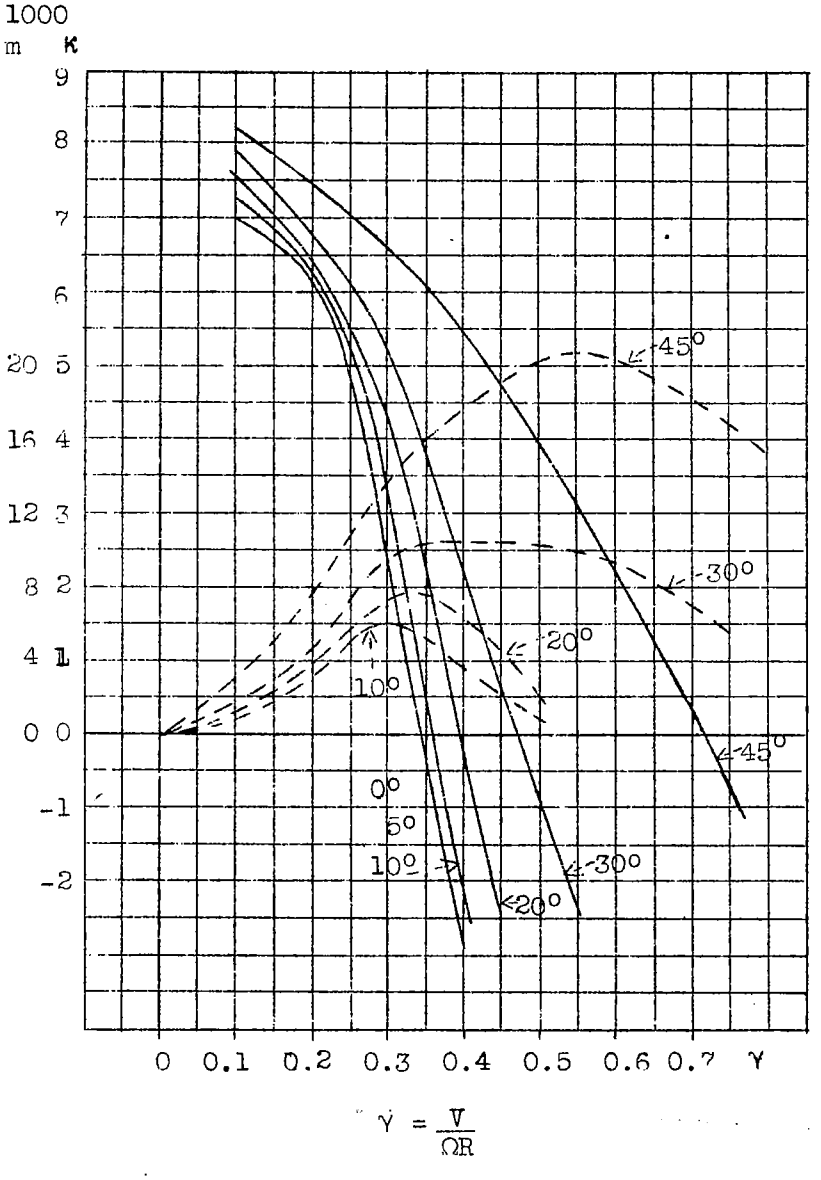

Figure 5.- Yaw tests, 2-blade metal propeller, Torino E 1. p/D= 0.9

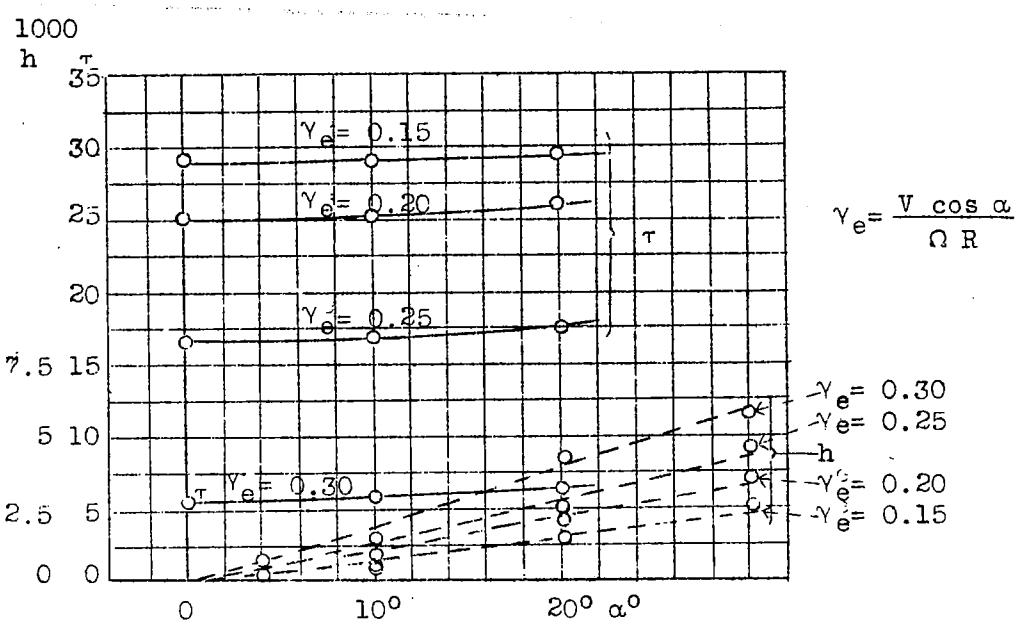

Figure 6.

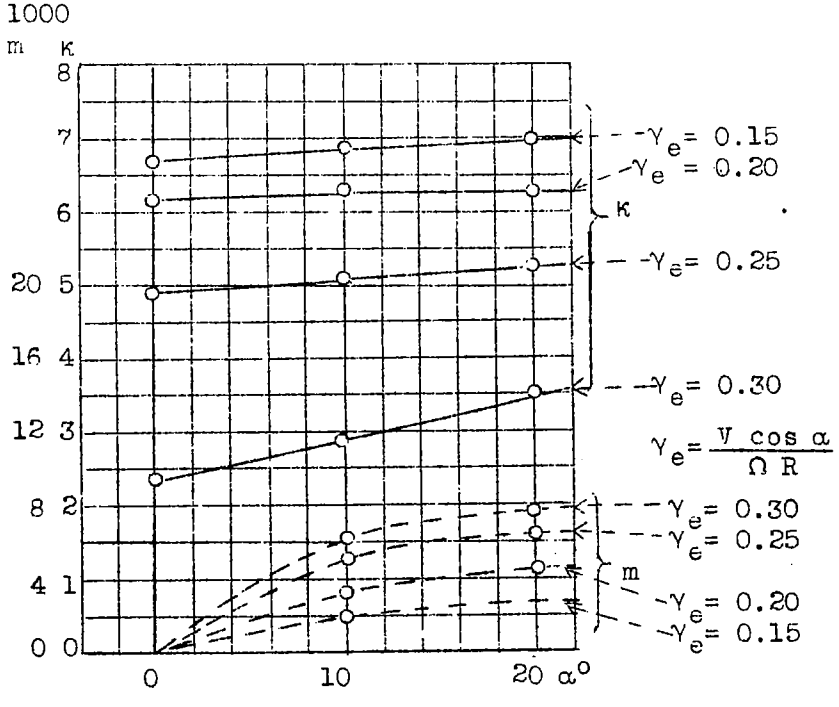

Figure 7.
Yaw tests, 2-blade metal propeller. Torino E 1. p/D= 0.9

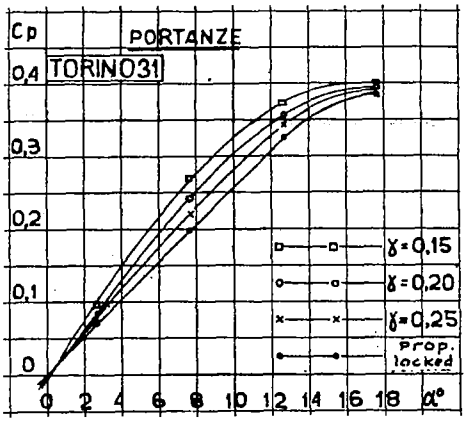

Figure 9.- Lift curves of tail of triangular plan form , Torino 31. Angle of tail setting 0°. p/D=0.9

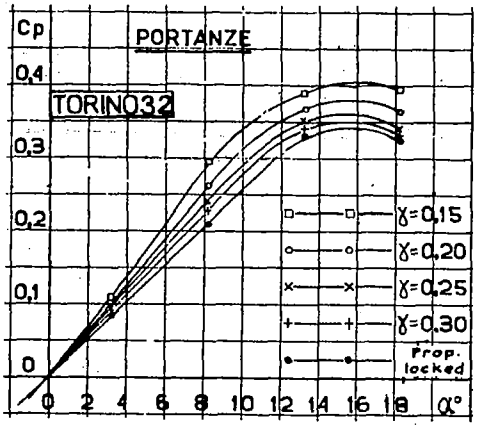

Figure 10.- Lift curves of tail of elliptical plan form. Torino 32. Angle of tail setting 0°. p/D=0.9

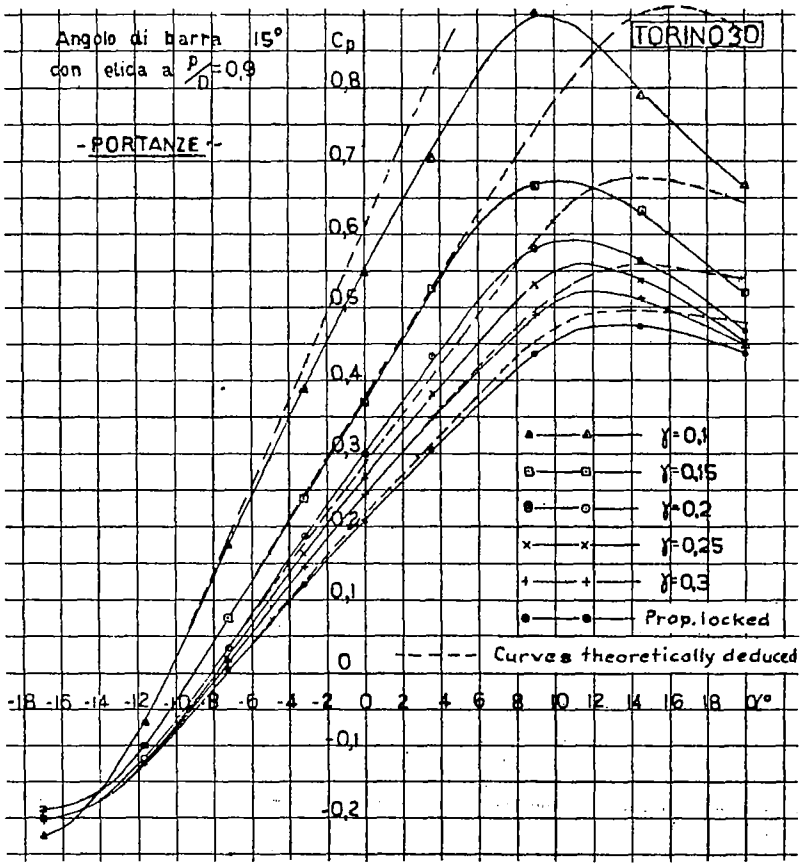

Figure 11.- Lift curves of rectangular tail. Torino 30, Angle of tail setting 15°. p/D=0.9

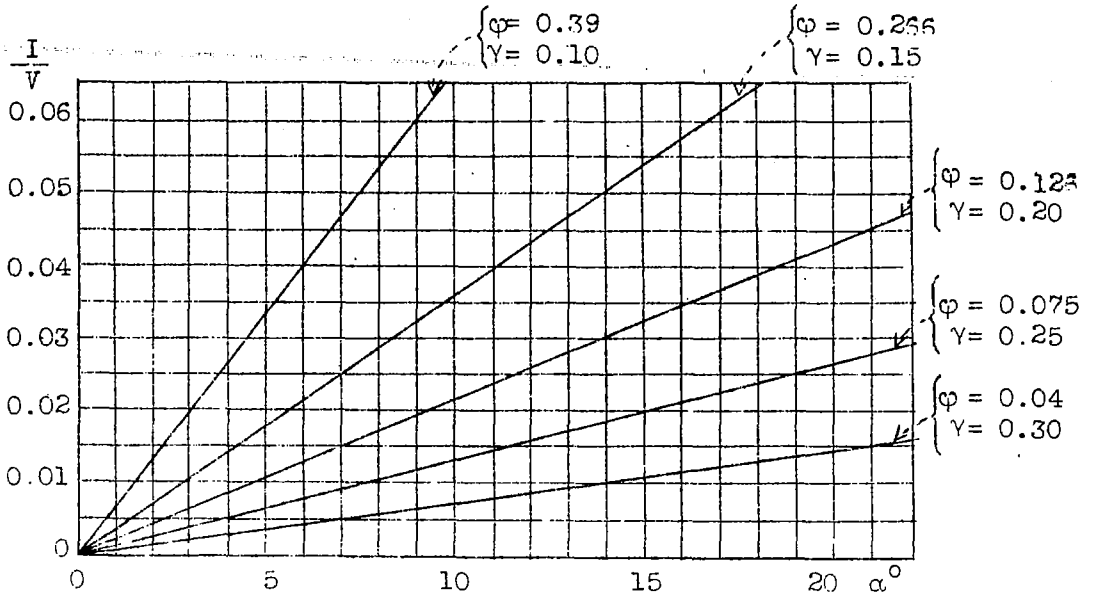

Figure 12.

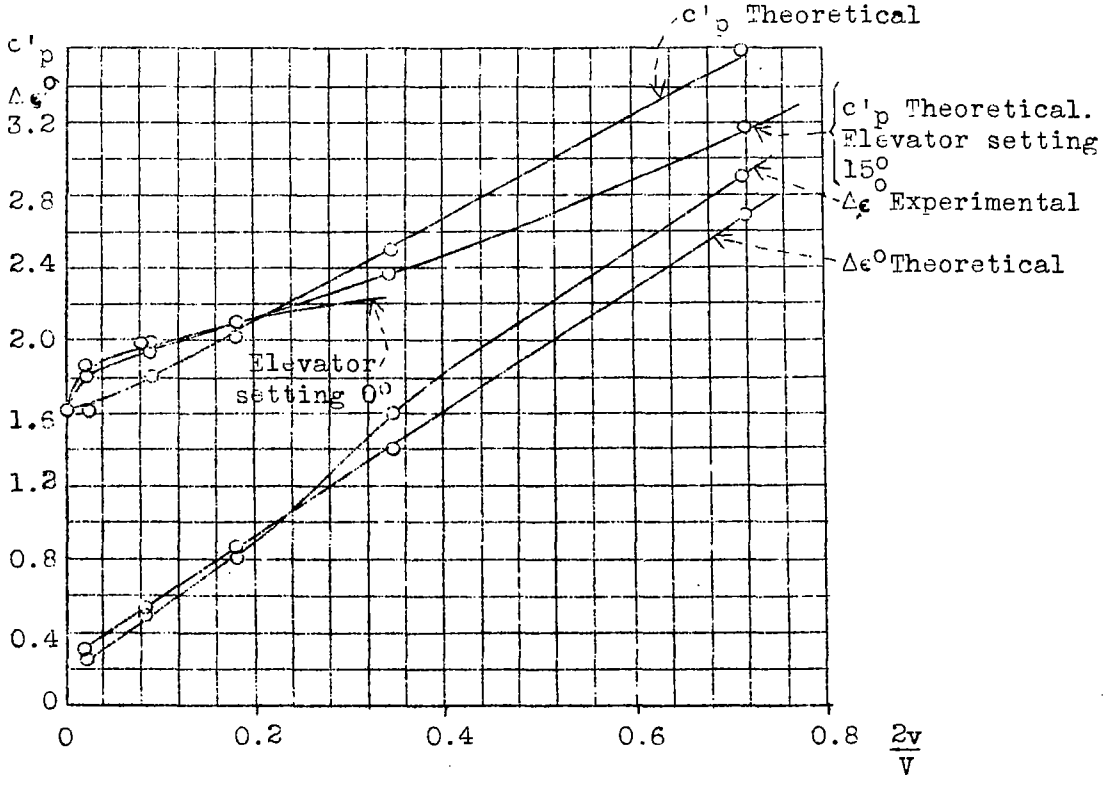

Figure 13.

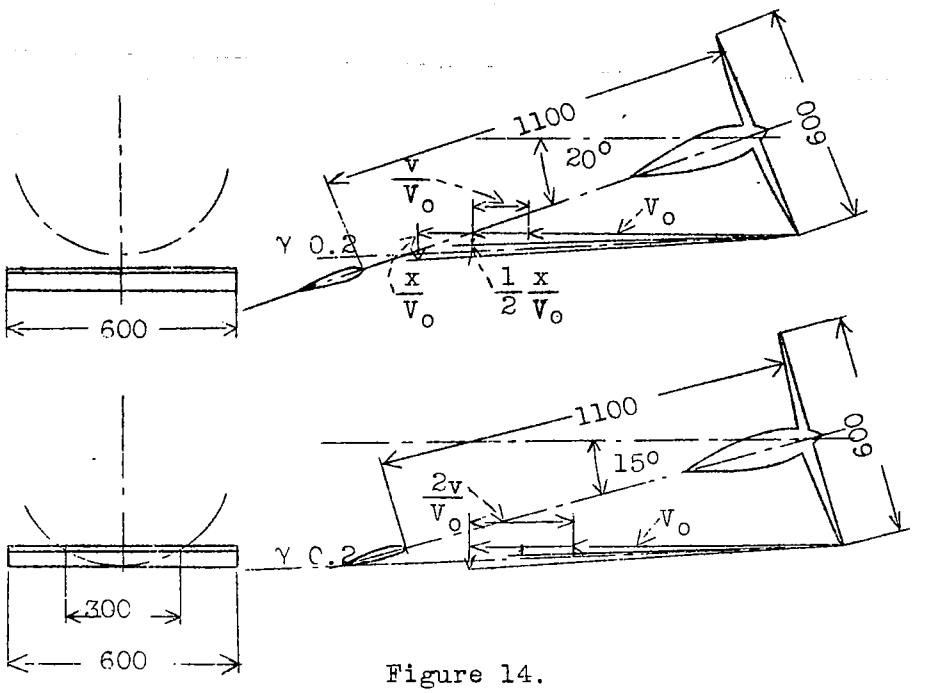

Figure 14.

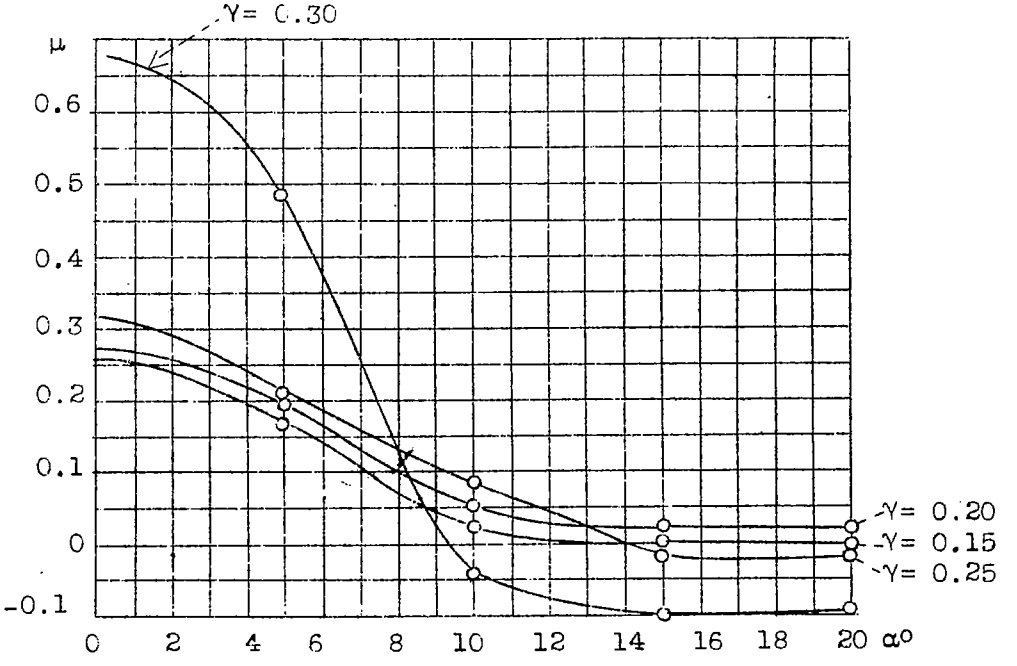

Figure 19

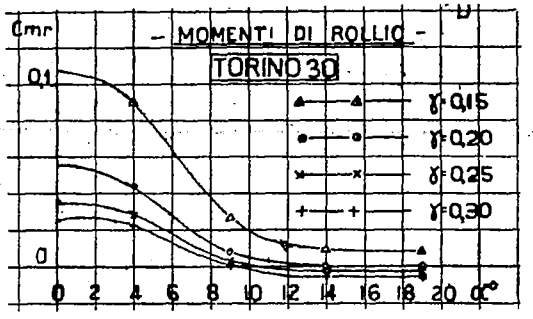

Figure 15.- Rolling-moment curves of tail of rectangular plan form . Torino 30. Angle of tail setting 0°. p/D=0.9

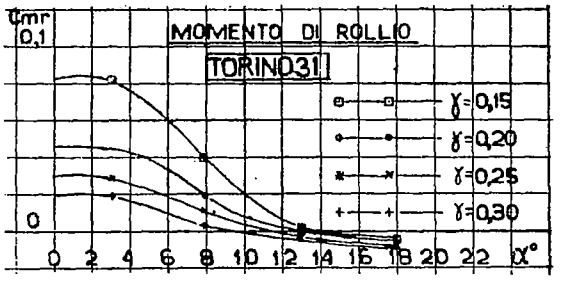

Figure 16.- Rolling-moment curves of tail of triangular plan form. Torino 31. Angle of tail setting 0°. p/D=0.9

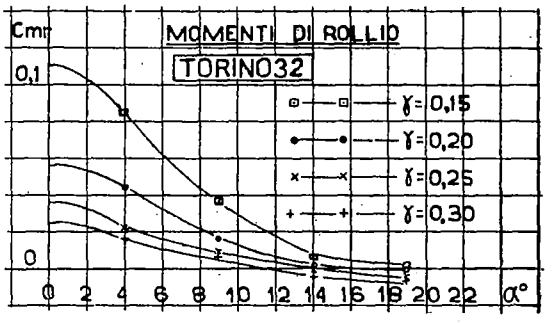

Figure 17.- Rolling-moment curves of tail of elliptical plan form. Torino 32. Angle of tail setting 0°. p/D=0.9

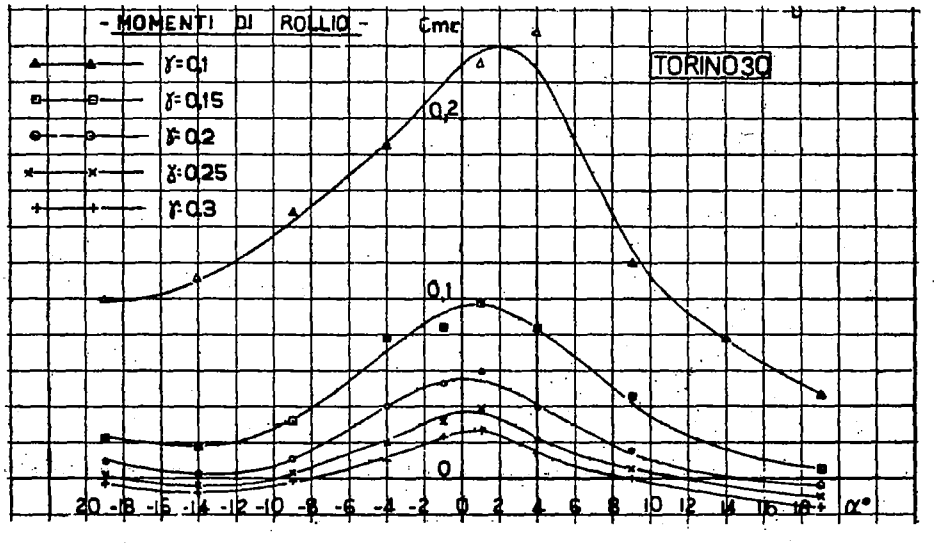

Figure 18.- Rolling-moment curves of tail of rectangular plan form. Torino 30. Angle of tail setting 15°. p/D=0.9